AIAA 82-4214

Effect of Unsteady Forcing on the Sinusoidal Instability of Vortex Wakes

Donald B. Bliss*
Princeton University, Princeton, N.J.

An analytical model of the vortex wake instability subject to forcing by unsteady lift fluctuations has been developed. These lift fluctuations can be caused either by variations in angle of attack or by flying through atmospheric turbulence. The effect of turbulence in the fluid itself, already studied by Crow and Bate, has been reviewed and incorporated into the analysis. A simple procedure is provided to estimate the time at which contact occurs between the two wake vortices as a function of certain characteristics of the forcing inputs. The behavior of the instability is somewhat altered by these forcing terms. In particular, it was found that contact between vortices can occur at much shorter wavelengths than predicted for the unforced case. Furthermore, in the presence of forcing, the minimum completion time for the instability does not correspond to the wavenumber for which the amplification rate is a maximum because the length of the vortex trajectories is also an important factor. Finally, the stability boundary is extended to larger wavenumbers by the presence of forcing, and the boundary location depends on the forcing level.

Introduction

IT is now well known that the trailing vortex pair produced by a lifting surface undergoes a coupled sinusoidal deformation. The sinusoidal instability grows until the cores of the two vortices come into contact, often causing the pattern to break up into crude rings. It is of both fundamental and practical interest to understand the factors which affect the growth rate of this vortex wake instability since it is the first step in a complex series of events which cause the wake to dissipate.

The instability, which was first studied theoretically by Crow,[1] involves a balance between the mutual interaction of the deformed vortices and the self-induced motion due to curvature of the vortex filaments. The original analysis by Crow used an undetermined cut-off distance in the evaluation of the Biot-Savart law in order to avoid a singularity in the calculation of the self-induced motion. Shortly thereafter, Bliss[2] and Widnall, Bliss, and Zalay[3] analyzed the self-induced motion of a curved rotational vortex core of finite size. This analysis showed that the self-induced motion could be determined in terms of the circulation, core size, radius of curvature, and integrals of the swirl and axial velocity distributions in the vortex core. As a convenience, a formula was derived to allow the correct value for the cut-off distance to be chosen.[2] Similar results were also obtained by Moore and Saffman.[4]

Using the analysis of the self-induced motion of finite size cores, Bliss[2] and Widnall, Bliss, and Zalay[3] reexamined the sinusoidal instability problem, and the functional dependence of the amplification rate on the actual vortex core properties was determined. This analysis was also used to solve some other vortex motion problems, including the determination of the speed of a vortex ring[2,3] and the stability of helical vortex filaments.[5] Widnall and Bliss[6] also incorporated the analysis of self-induced motion into a slender body theory for the motion of vortex wakes. This method allowed the inclusion of very large axial velocities in the vortex core. In addition, it showed that a great deal of useful information could be learned from a relatively simple force balance approach.

Two additional factors which can affect the growth rate of the sinusoidal instability are the subject of this report. These factors are unsteady wing loading and the presence of disturbances in the flowfield. Each of these effects has already received some attention, as described below.

The effect of an unsteady load distribution was investigated by Bilanin and Widnall[7] for the case of constant net lift. The effect of differentially operated flaps was studied theoretically and experimentally and was shown to be a possible means of hastening the completion of the sinusoidal instability. Chevalier[8] showed in flight tests that periodic angle-of-attack variations forced the instability and reduced the time required for the vortices to come into contact. Apparently the important case of varying the net lift has not yet been studied theoretically. In practice, load variations could arise either by the lifting surface encountering disturbances or by continual corrective motions applied by the pilot.

The effect of turbulence in the fluid in which the sinusoidally deforming wake is embedded was investigated by Crow and Bate.[9] The cases of very strong and very weak turbulence levels were considered and the results were used to form a composite curve for the wake lifespan (defined statistically) as a function of the turbulent energy dissipation rate. The turbulent eddies were assumed to lie in the Kolmogorov inertial subrange. The results show that the presence of turbulence will reduce the mean lifespan of the vortex wake, however the effect is relatively weak for low turbulence levels. Portions of the present work reflect the influence of Ref. 9.

The present study has a somewhat different emphasis than the earlier basic work on the sinusoidal instability,[1-3,6] which had as a major concern the identification of the underlying mechanism and the prediction of the amplification rate and stability boundaries. The present work builds on the previous results and seeks to describe the factors which force or provide initial conditions for the instability. Characterization of these factors allows the prediction of a definite time for the instability to go to completion. The result is therefore more precise than simply saying that the instability goes to completion in a time on the order of the time scale associated with the amplification rate. Furthermore, the relative importance of the various factors which force the instability can be compared. This approach has also been taken in Refs. 7 and 9.

Basic Sinusoidal Instability

The basic configuration of the symmetric mode of the sinusoidal instability is shown in Fig. 1. An asymmetric mode is also possible but is not of practical importance. The instability proceeds with each vortex lying in a tipped plane, at

Received March 9, 1981; revision received Oct. 13, 1981.

*Assistant Professor, Department of Mechanical and Aerospace Engineering.

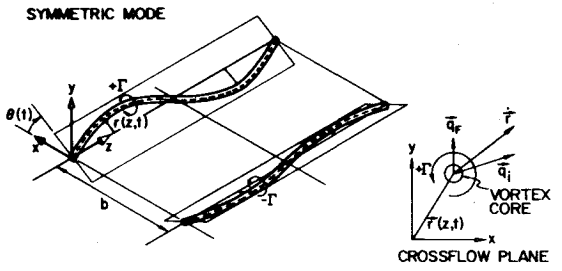

Fig. 1 General features of the vortex pair instability.

least as long as nonlinear terms can be neglected. In its simplest form the instability involves a balance between the mutual induction of the opposing deformed vortices and the self-induced motion of each sinusoidally curved vortex. An isolated sinusoidal vortex rotates rigidly without shape change at a rate dependent on the circulation, the wavelength, and the vortex core size and energy content. In the vortex pair instability, this rotation is balanced by the mutual induction velocity field of the opposing vortex, which depends on the circulation, wavelength, and spacing. Under the condition of rotational equilibrium, there is an unbalanced radial velocity associated with the mutual induction which causes the amplitude of the sinusoid to grow exponentially. If the starting point of the tipped planes is not at the orientation for rotational equilibrium, then both the orientation and amplitude of the sinusoid change as a function of time.

The mutual induction velocity field can be calculated in a straightforward manner by applying the Biot-Savart law to sinusoidally deformed line vortices.[1] The Biot-Savart law is not adequate to calculate the self-induced velocity of a curved vortex filament, because the integral diverges when the point of evaluation is on the vortex itself. This difficulty can be overcome by considering the fluid mechanics of the actual curved vortex core, using the method of matched asymptotic expansions.[2,3] The effect of the vortex core properties can be incorporated subsequently into a "cut-off" distance at which the Biot-Savart integral is stopped on either side of the point of evaluation, such that the correct answer is obtained.[2,4]

It has been shown that the motion of the vortices can be treated in terms of velocity components in a cross-flow plane.[6,7] The same simple approach will be taken to develop the results of the present study. Referring to Fig. 1, the nondimensional displacement of the vortex core in the cross-flow plane is

$$r=(xi+yj)e^{i\hat{k}z} \tag{1}$$

where x and y are perturbation amplitudes nondimensionalized by the average vortex spacing b. The distance z along the wake is similarly nondimensionalized, and the nondimensional wavenumber is $\hat{k}=2\pi b/\lambda$. The vector equation of motion of the basic instability is

$$\frac{\mathrm{d}r}{\mathrm{d}t}=q_i(r) \tag{2}$$

where q_i is the resultant vector of the mutual and self-induced velocities. This velocity is nondimensionalized by $\Gamma/2\pi b$ and the time is nondimensionalized by $2\pi b^2/\Gamma$, where Γ is the circulation. It is found that

$$q_i(r)=[Xxj+Yyi]e^{i\hat{k}z} \tag{3}$$

where X and Y are the nondimensional velocity coefficients associated with displacements x and y. The formulas for the coefficients are[6]

$$X=1+\hat{k}K_1(\hat{k})-\Omega_0 \tag{4}$$

$$Y=1-\hat{k}^2K_0(\hat{k})-\hat{k}K_1(\hat{k})+\Omega_0 \tag{5}$$

where Ω_0 is the nondimensional self-induced rotation of a sinusoidal vortex. In Eqs. (4) and (5) the constant, unity, is associated with the displacement of one vortex in the zeroth-order strain field of the other. The terms involving the modified Bessel functions of the first kind are associated with the displacement of the opposing vortex.

The formula for the self-induced rotation, valid only for $ka_e \ll 1$, is

$$\Omega_0=\tfrac{1}{2}\hat{k}^2\{-\ell n[\hat{k}a_e/b]+\ell n2-\gamma_e\} \tag{6}$$

where $\gamma_e=0.5772...$ is Euler's constant and a_e is an effective core size.

$$a_e=ae^{-(A-C)} \tag{7}$$

where a is the actual core radius, or an associated length scale, and the constants A and C are related to the kinetic energy in the vortex core associated with the swirl and axial velocity components, respectively.[2,3] Most generally,

$$A=\lim_{\bar{r}\to\infty}\left[\int_0^{\bar{r}}\bar{r}v_0^2\mathrm{d}\bar{r}-\ell n\bar{r}\right] \tag{8}$$

where $\bar{r}=r/a$, and $v_0(\bar{r})$ is the swirl velocity distribution in the vortex core nondimensionalized by $\Gamma/2\pi a$. Similarly, if W_A is the total kinetic energy per unit length associated with axial velocity in the vortex core, then

$$C=\frac{8\pi}{\rho\Gamma^2}W_A=\int_0^{\infty}2\bar{r}w_0^2\mathrm{d}\bar{r} \tag{9}$$

where $w_0(\bar{r})$ is the axial velocity distribution in the vortex nondimensionalized by $\Gamma/2\pi a$. It is helpful to give the value of A for two vortex cores of interest. For the constant vorticity core a simple calculation gives $A=0.25$. For a "decaying" vortex core based on the similarity solution for viscous diffusion of a point vortex (here $a=\sqrt{4\nu t}$), a more difficult calculation gives $A=-0.058$. Typically, C will also be a number of order unity or smaller. The important conclusion is that a_e is of the same order as the actual core size.

Returning to the problem formulation, notice that Eqs. (2) and (3) can be combined and rewritten as

$$\frac{\mathrm{d}}{\mathrm{d}t}\begin{bmatrix}x\\y\end{bmatrix}=\begin{pmatrix}0 & Y\\ X & 0\end{pmatrix}\begin{bmatrix}x\\y\end{bmatrix} \tag{10}$$

or simply as

$$\frac{\mathrm{d}r}{\mathrm{d}t}=\underset{\sim}{A}\,r \tag{11}$$

As posed, the solution of this problem is completely specified once an initial condition $r^0=x_0i+y_0j$ is given. This corresponds to specifying an initial orientation angle, $\theta_0=\tan^{-1}(y_0/x_0)$, and amplitude, $r_0=\sqrt{x_0^2+y_0^2}$, of the sinusoid. However, the current interest centers on the inclusion of other factors affecting the instability. The solution of Eq. (11) is therefore deferred until later when these factors can be added as nonhomogeneous forcing terms to the equation, giving the following form

$$\frac{\mathrm{d}r}{\mathrm{d}t}=\underset{\sim}{A}\,r+q_F \tag{12}$$

Here the velocity vector q_F is the forcing associated the effects of unsteady loading on the lifting surface and the presence of disturbances imbedded in the fluid. The expressions for these contributions will be developed in subsequent sections.

Underlying Assumptions

Several basic assumptions are set down in this section which lead to substantial simplifications in the analysis that follows. Although most of these assumptions could be avoided at the expense of a considerable increase in complexity, there is no reason to believe that a significant improvement in accuracy or confidence would be obtained. In other words, the present study is a consistent engineering analysis of the problem.

First, it will be shown that the wake is laid down quickly compared to the time scales associated with the instability. This fact allows the actual process to be modeled as a vortex pair instability in which disturbances are periodic and the effects of spatial variations along the wake are neglected. This assumption has also been made in all previous analyses, but is particularly important to provide verification when forcing terms are present.

The time scale associated with the basic (unforced) instability is $T_b = 2\pi b^2/\Gamma$. In this time, the lifting surface moving at speed U has traveled a distance $d_l = UT_b$. Assuming elliptical loading, the circulation can be related to the lift coefficient by the relation

$$\tfrac{1}{2}\rho U^2 (b_s^2/\mathcal{R}) C_L = (\pi/4)\rho U \Gamma b_s \tag{13}$$

where b_s is the span and $\mathcal{R}$ is the aspect ratio. For elliptical loading $b = (\pi/4) b_s$. Solving for Γ and substituting gives

$$d_l/b = (\pi^3/4)(\mathcal{R}/C_L) \gg 1 \tag{14}$$

Typically, this ratio will be $0[10^2]$ or larger. Thus the lifting surface will have traveled many vortex spacings during the first e-folding time of the instability.

Some additional consideration is required when the instability is forced. If the magnitude of the forcing velocity is v_F, then the ratio v_F/U must be small for the assumption to hold. When the forcing is due to turbulence or waves in the fluid then the velocity components associated with these disturbances must be small compared to the flight speed. When the forcing is caused by load variations on the lifting surface, then $v_F \approx \Delta\Gamma/2\pi b$, where $\Delta\Gamma$ is the variation in circulation. Using Eq. (13), the ratio of velocities for the varying load case is

$$\frac{v_F}{U} = \left(\frac{4}{\pi^3}\frac{C_L}{\mathcal{R}}\right)\frac{\Delta\Gamma}{\Gamma} \ll 1 \tag{15}$$

The condition is easily satisfied since the term in parentheses is $0[10^{-2}]$ and typically $\Delta\Gamma/\Gamma \ll 1$ (for reasons discussed later in this section).

The above discussion shows that even in the presence of a disturbance velocity field the wake can be assumed to be initially flat. Any initial variation in the vertical displacement of the wake can be ascribed to vertical motion of the lifting surface itself as the wake is being laid down. However, initial horizontal displacements of the wake will occur if there are changes in the spanwise load distribution on the lifting surface.

Load distribution changes may be caused by the motion of control surfaces, by built-in twist when the angle of attack changes, and by unsteady effects. It will now be shown that, for the sinusoidal instability, load variations due to unsteady effects are not important. The Strouhal number based on mean chord is $S_t = f_u \bar{c}/U$. The mean chord can be written in terms of the span and the aspect ratio: $\bar{c} = b_s/\mathcal{R}$. The frequency expressed in terms of the wavelength λ of disturbances in the wake is $f_u = U/\lambda$; then $S_t = b_s/(\mathcal{R}\lambda) \ll 1$. The Strouhal number is small because the aspect ratio is typically greater than unity, and because the most unstable wavelengths for sinusoidal instability are typically several times the span. When the Strouhal number is much less than unity, the aerodynamic behavior of the wing is quasi-steady and there are no significant changes in load distribution due to unsteady effects.

For the purpose of this work, the trailing vortices are assumed to be laid down as straight lines, i.e., initial vertical and horizontal displacements due to vehicle motion and changing load distribution are not considered. These effects are easily included in the initial conditions once a specific planform and its longitudinal dynamics are specified. They will not, however, introduce any fundamental changes in the results. The important conclusion arising from this discussion is that specific initial conditions can be deduced for the sinusoidal instability. This fact allows the prediction of a definite completion time to be made. For the rest of this work, zero initial displacements are assumed as the initial condition.

A linearized analysis is used in this study to predict the completion time. This approach is supported by the work of Ref. 10, in which the finite amplitude effects in the mutual induction terms† were included in a numerical study of the instability. A comparison was made showing that the linear theory was capable of predicting the completion time with reasonable accuracy. In addition, there is also some experimental evidence which supports this assumption.[9,11] Apparently, the nonlinear effects act only over the last fraction of the wake lifetime, and do not dramatically affect the growth rate.

A related assumption is that all the forcing terms act as small perturbations on the mean state and the product of any two perturbation terms is negligible. In particular, when the lifting surface undergoes unsteady loading, the condition $\Delta\Gamma/\Gamma \ll 1$ is assumed to hold and the product of this quantity and any other small quantity, e.g., the instability amplitude, is assumed to be negligible. This restriction is not strictly necessary in the context of a linear analysis, but it has the advantage of introducing substantial simplifications. It is, in fact, unlikely that a consistent analysis can be constructed when the products of $\Delta\Gamma/\Gamma$ and amplitude-dependent quantities are retained, since it can be argued that a great deal more structural information about the basic wake must then be known. For instance, the location of the cross-sheet of shed vorticity would have to be determined more precisely.

Actually, the case of $\Delta\Gamma/\Gamma \ll 1$ is very important since it leads to the longest predicted completion times. It is also the most physically realistic case, since it is neither common nor desirable to operate an aircraft with large periodic variations of the net lift. Indeed, it is clear that when $\Delta\Gamma/\Gamma \simeq 1$, the wake lifetime will be very short. In this case a continuous wake is not formed since the two trailing vortices link together each time the net circulation vanishes. The initial configuration of such a wake will then resemble the final configuration of a normal wake after the completion of sinusoidal instability. Further dissipation of the wake then occurs by some other mechanism.

Effect of Unsteady Loading

The induced velocity on a trailing vortex due to unsteady loading on the lifting surface arises from the variation in circulation along the opposite vortex and from the cross-sheet of spanwise shed vorticity. For clarity, the derivation in this section is carried out in dimensional variables. The circulation along the trailing vortex passing through the origin in Fig. 2 is

$$\Gamma_t = \Gamma + \Delta\Gamma e^{ikz} \tag{16}$$

where it is assumed that $\Delta\Gamma/\Gamma \ll 1$. The wavenumber is determined by the relation $k = 2\pi f_u/U$, where f_u is the frequency of the load variation. From the conservation of

†The linear self-induction term is valid as long as the core size is small compared to the radius of curvature, never a serious restriction for the sinusoidal instability.

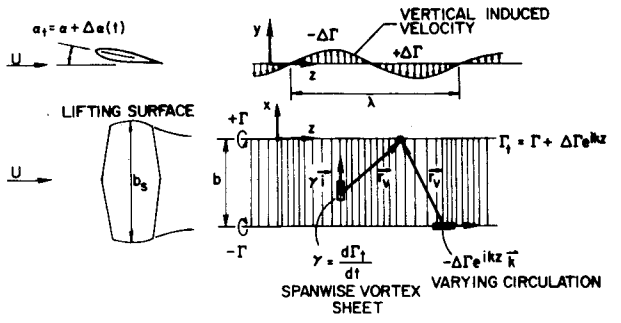

Fig. 2 Geometry for calculating the forcing velocity due to unsteady loading.

vorticity, it then follows that the circulation per unit length of the cross sheet is

$$\gamma = \frac{d\Gamma_t}{dz} = ik\Delta\Gamma e^{ikz} \tag{17}$$

In the present analysis, which neglects the products of small quantities, the vortex sheet can be assumed to be flat, and the varying component of circulation in the opposite vortex can be located at the unperturbed position. The induced velocity contributions of these two effects can now be calculated. Figure 2 shows the geometry for determining the effect of the circulation variation along the opposite vortex. In general, the Biot-Savart law is expressible as a volume integral over the vorticity distribution:

$$u = \frac{1}{4\pi}\int_V \frac{\zeta \times r_v}{r_v^3} dV \tag{18}$$

where r_v is the vector distance from the element of vorticity to the point at which the velocity is to be computed. For the present case the velocity variation due to the varying circulation along the opposite vortex is

$$u_v = \frac{1}{4\pi}\int_{-\infty}^{+\infty} \frac{-\Delta\Gamma e^{ikz_1} i \times (ib + [z - z_1]k)}{[(z-z_1)^2 + b^2]^{3/2}} dz_1 \tag{19}$$

In a straightforward manner this reduces to

$$u_v = -j\frac{(kb)^2\Delta\Gamma}{4\pi b} e^{ikz}\int_{-\infty}^{+\infty} \frac{\cos s + i\sin s}{[s^2 + (kb)^2]^{3/2}} \tag{20}$$

where $s = k(z_1 - z)$. The imaginary part of the integral is zero because that portion of the integrand is an odd function. The remaining term can be evaluated as a Fourier cosine transform[12] to give

$$u_v = -j\frac{\Delta\Gamma}{2\pi b} e^{ikz}(kb)K_1(kb) \equiv j\frac{\Gamma}{2\pi b}\frac{\Delta\Gamma}{\Gamma} V_v(kb)e^{ikz} \tag{21}$$

where K_1 is a modified Bessel function of the first kind. The function $V_v(kb)$ is plotted in Fig. 3.

The geometry to evaluate the velocity induced by the cross sheet is also shown in Fig. 2. The Biot-Savart law becomes

$$u_c = \frac{1}{4\pi}\int_{-\infty}^{+\infty}\int_{-b}^{0} \frac{\gamma(z_1) i \times (-ix_1 + [z - z_1]k)}{[(z-z_1)^2 + x_1^2]^{3/2}} dx_1 dz_1 \tag{22}$$

Substituting Eq. (17) and integrating over the width gives

$$u_c = -j\frac{i(kb)\Delta\Gamma}{4\pi}\int_{-\infty}^{+\infty} \frac{e^{ikz_1}}{(z-z_1)[(z_1-z)^2 + b^2]^{1/2}} dz_1 \tag{23}$$

This integral is then reexpressed in terms of the variable $s = k(z_1 - z)$. The resulting term associated with the real part

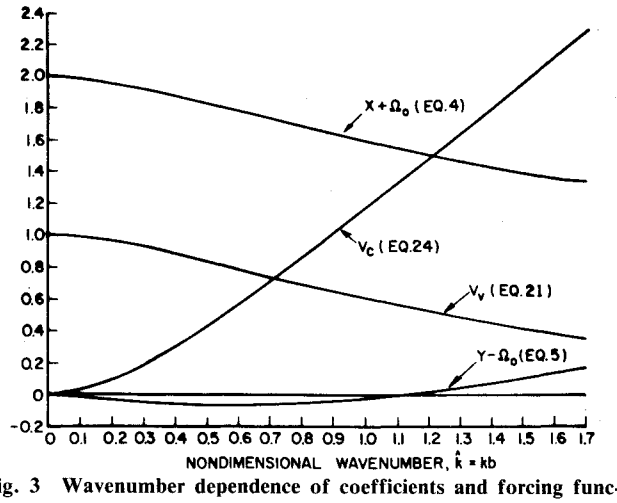

Fig. 3 Wavenumber dependence of coefficients and forcing functions.

of the integrand vanishes because the function is odd. The induced velocity associated with the cross sheet is therefore given by

$$u_c = -j\frac{\Delta\Gamma}{2\pi b}(kb)^2 e^{ikz}\int_0^{+\infty} \frac{\sin s}{s[s^2 + (kb)^2]^{1/2}} ds$$

$$\equiv j\frac{\Gamma}{2\pi b}\frac{\Delta\Gamma}{\Gamma} V_c(kb)e^{ikz} \tag{24}$$

The function $V_c(kb)$ was evaluated numerically and is shown in Fig. 3.

The two velocity vectors associated with unsteady loading, u_v and u_c, do not depend on the amplitude of the instability. Therefore they act as constant forcing terms in the governing equation for the vortex instability. Note that the angle-of-attack variation, $\Delta\alpha$, required to produce a circulation change, $\Delta\Gamma$, is given by $\Delta\alpha/\alpha = \Delta\Gamma/\Gamma$, where Γ is given by Eq. (13) for an elliptical load distribution.

The effects of unsteady loading can be combined and expressed as

$$u_u = j(\Gamma/2\pi b)Q_u e^{ikz} \tag{25}$$

where the nondimensional velocity amplitude is

$$Q_u \equiv (\Delta\Gamma/\Gamma)(V_v + V_c) \tag{26}$$

Finally, it should be noted that the variation in circulation associated with unsteady loading does not affect the self-induced velocity in the present analysis because of the assumption that $\Delta\Gamma/\Gamma \ll 1$, and because terms involving the product of $\Delta\Gamma/\Gamma$ and the instability amplitude are neglected.

Effect of Fluid Disturbances

Suppose that a spatially periodic velocity disturbance field is imbedded in the fluid. Such a disturbance field can affect the sinusoidal instability in two ways. As the lifting surface travels through the disturbance it will experience unsteady loading due to angle-of-attack variations. This effect was covered in the previous section. The disturbance field can also force the sinusoidal instability directly. Since the most unstable wavelength of the basic instability is on the order of several separation distances,[3] it is expected that only relatively large-scale disturbances will play an important role in forcing the instability. In fact, for wavelengths shorter than a critical value, the wake is "stable" and the individual perturbed vortices rotate under their own self-induction.[1,3,6,9] In addition, since excitation of the symmetric mode is of interest, only the mean vertical velocity component at each station along the wake need be considered. This is the approach taken by Crow and Bate,[9] who considered this aspect of the

problem previously to determine the response to atmospheric turbulence. They employed the assumption that the velocity field can be modeled as frozen, or time independent, because the time scale associated with large eddies would be long compared to the instability time scale.

For the present work the disturbance velocity field is written as

$$u_d = j(\Gamma/2\pi b)\,Q_d(t)\,e^{ikz} \tag{27}$$

where $Q_d(t)$ is a time-dependent disturbance amplitude nondimensionalized by the wake velocity scale $\Gamma/2\pi b$. In particular, the case of harmonic time dependence will be considered, namely,

$$Q_d(t) = V_d e^{i\omega t} \tag{28}$$

where the magnitude of the constant V_d is the amplitude of the disturbance and will in general be a function of the frequency and wavenumber. This form reduces to the case of a time-independent velocity field when $\omega = 0$.

Prediction of the Completion Time

All the elements necessary to pose and solve the problem of forced sinusoidal instability are now available. The nondimensional velocity vector q_F, which forces the instability in Eq. (12), is specified using Eqs. (25) and (27):

$$q_F = Q_u j + Q_d j \tag{29}$$

Using Eqs. (10), (12), (26), (28), and (29), the nondimensional equation is

$$\frac{d}{dt}\begin{bmatrix} x \\ y \end{bmatrix} = \begin{bmatrix} 0 & Y \\ X & 0 \end{bmatrix}\begin{bmatrix} x \\ y \end{bmatrix} + Q_u \begin{bmatrix} 0 \\ 1 \end{bmatrix} + V_d \begin{bmatrix} 0 \\ 1 \end{bmatrix} e^{i\omega t} \tag{30}$$

Equation (30) is a system of two nonhomogeneous, constant coefficient, first-order equations. The solution of such a system is straightforward.[13] The roots of the characteristic equation are found to be $r_{1,2} = \pm\sqrt{XY}$, and the corresponding eigenvectors are $\xi^{1,2} = \sqrt{Y}\,i \pm \sqrt{X}\,j$. The particular solution is conveniently found by either the method of undetermined coefficients or by reduction of order. The general solution is then required to satisfy the initial condition $r(0) = r^0 = x_0 i + y_0 j$. The result is

$$\begin{bmatrix} x \\ y \end{bmatrix} = \begin{bmatrix} x_0 \\ y_0 \end{bmatrix}\cosh\sqrt{XY}t + \begin{bmatrix} y_0\sqrt{Y/X} \\ x_0\sqrt{X/Y} \end{bmatrix}\sinh\sqrt{XY}t + Q_u/X \begin{bmatrix} \cosh\sqrt{XY}t - 1 \\ \sqrt{X/Y}\sinh\sqrt{XY}t \end{bmatrix} + \frac{V_d}{XY+\omega^2}\left\{\begin{bmatrix} Y \\ i\omega \end{bmatrix}(\cosh\sqrt{XY}t - e^{i\omega t}) + \begin{bmatrix} i\omega\sqrt{X/Y} \\ Y\sqrt{X/Y} \end{bmatrix}\sinh\sqrt{XY}t\right\} \tag{31}$$

As explained in the section on underlying assumptions, for the present work the initial conditions $x_0 = y_0 = 0$ will be used. There is no special difficulty with nontrivial initial conditions, once they are specified, since the solution has been found. The two types of forcing will be considered independently.

Suppose the lifting surface is subject to periodic unsteady loading as it travels through a uniform undisturbed fluid ($V_d = 0$). The amplitude factor Q_u is determined using Eqs. (26), (21), and (24) once the normalized wavenumber, $k = kb$, and circulation perturbation, $\Delta\Gamma/\Gamma$, are known. As long as $XY > 0$ the components of the wake displacement are given by

$$x = (Q_u/X)\,(\cosh\sqrt{XY}t - 1) \tag{32a}$$

$$y = (Q_u/\sqrt{XY})\sinh\sqrt{XY}t \tag{32b}$$

The angle of the tipped plane containing the vortex is given by

$$\theta(t) = \tan^{-1}\sqrt{Y/X}\,\frac{\sinh\sqrt{XY}t}{\cosh\sqrt{XY}t - 1} \tag{33}$$

so that $\theta(0) = 90$ deg and $\theta(t) \to \tan^{-1}\sqrt{Y/X}$ as t becomes large. Thus the tipped planes containing the wake are initially vertical and rotate to approach a fixed tilt angle asymptotically. The vortex trajectory described by Eq. (32) is a hyperbola. The vortex motion in the cross-flow plane is illustrated schematically in Fig. 4. The angle that is approached is the same as that approached by an unforced sinusoidal instability with nonzero initial conditions.

For the present discussion, the completion time t_c is defined as the time at which the centers of the opposing vortices coincide, namely, $x(t_c) = \frac{1}{2}$. This definition may be somewhat conservative for vortices with large rotational cores, but there is uncertainty in any event owing to the period of nonlinear interaction between the vortices. Then, using Eq. (32a), the completion time is

$$t_c = (1/\sqrt{XY})\cosh^{-1}[(X/2Q_u) + 1] \tag{34}$$

This result applies for the case of $XY > 0$. When $Q_u \ll 1$ and $X = 0$[1], then the above expression simplifies to

$$t_c \simeq (1/\sqrt{XY})\,\ell n[X/Q_u] \tag{35}$$

This result will become increasingly accurate as $\Delta\Gamma/\Gamma$ decreases, since Q_u is proportional to this factor. The important point is that the completion time increases roughly as

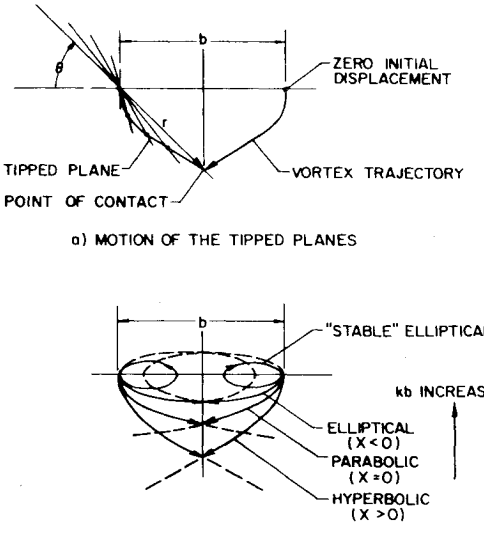

Fig. 4 Behavior of the forced vortex pair instability in the cross-flow plane.

the natural logarithm of $(\Delta\Gamma/\Gamma)^{-1}$. In other words, its dependence on disturbance amplitude is relatively weak.

The cases of $XY \leq 0$ must also be considered. An examination of the functions X and Y shows that, although Y remains positive, X becomes negative as $\hat{k}=kb$ is increased. In previous analyses, which considered an unforced vortex pair with nontrivial initial conditions, the occurrence of $X<0$ corresponded to a "stable" mode in which the sinusoidally disturbed vortices rotate about their axes and experience no net amplification. The behavior of the forced instability is different and somewhat more complicated.

Taking the limit as $X \to 0$, Eq. (32) becomes

$$x\Big|_{X=0} = (Q_u Y/2)t^2 \tag{36a}$$

$$y\Big|_{X=0} = Q_u t \tag{36b}$$

and the completion time is found to be

$$t_c = 1/\sqrt{Q_u Y} \quad \text{for} \quad X=0 \tag{37}$$

This result applies only at the one value of wavenumber for which $X=0$. The vortex trajectories are parabolas, as sketched in Fig. 4.

Equation (32) can be rewritten as follows when $X<0$:

$$x\Big|_{X<0} = (Q_u/X)(\cos\sqrt{-XY}t - 1) \tag{38a}$$

$$y\Big|_{X<0} = (Q_u/\sqrt{-XY})\sin\sqrt{-XY}t \tag{38b}$$

The completion time is given by

$$t_c = (1/\sqrt{-XY})\cos^{-1}[X/2Q_u + 1] \quad \text{for} \quad -2 < X/2Q_u < 0 \tag{39}$$

The trajectories are elliptical as indicated in Fig. 4. For the range of wavenumbers in which this result applies, the elliptical trajectories intersect and the instability can go to completion. For values of wavenumber such that $X/2Q_u < -2$, the elliptical trajectories do not intersect and the wake is "stable." Interestingly, the trajectory is quite different from that of the stable, unforced case.

Figure 5 shows curves of the completion time t_c as a function of the nondimensional wavenumber $\hat{k}$. Each curve is a line of constant disturbance amplitude $\Delta\Gamma/\Gamma$, and there is a different family of curves for each value of nondimensional vortex core size a_e/b. Comparison shows that the dependence on core size is relatively weak. The completion time of the sinusoidal instability forced by unsteady loading on the lifting surface is easily predicted from Fig. 5 once the requisite inputs are specified. The dimensional completion time is $t_{c_d} = (2\pi b^2/\Gamma)t_c$.

A similar set of results is obtainable when there is no unsteady loading ($Q_u = 0$) and the instability is forced by disturbances in the fluid. In this case Eq. (31) reduces to

$$x = \frac{V_d}{XY+\omega^2}\left[Y(\cosh\sqrt{XY}t - e^{i\omega t}) + i\omega\sqrt{Y/X}\sinh\sqrt{XY}t\right] \tag{40a}$$

$$y = \frac{V_d}{XY+\omega^2}\left[i\omega(\cosh\sqrt{XY}t - e^{i\omega t}) + Y\sqrt{Y/X}\sinh\sqrt{XY}t\right] \tag{40b}$$

Again the problem is to find t_c such that $x(t_c) = \frac{1}{2}$. Two cases are readily solvable.

Suppose first that $\omega = 0$ so that the fluid disturbance is time independent. The horizontal displacement of the vortex is then given by

$$x\Big|_{\omega=0} = (V_d/X)(\cosh\sqrt{XY}t - 1) \tag{41}$$

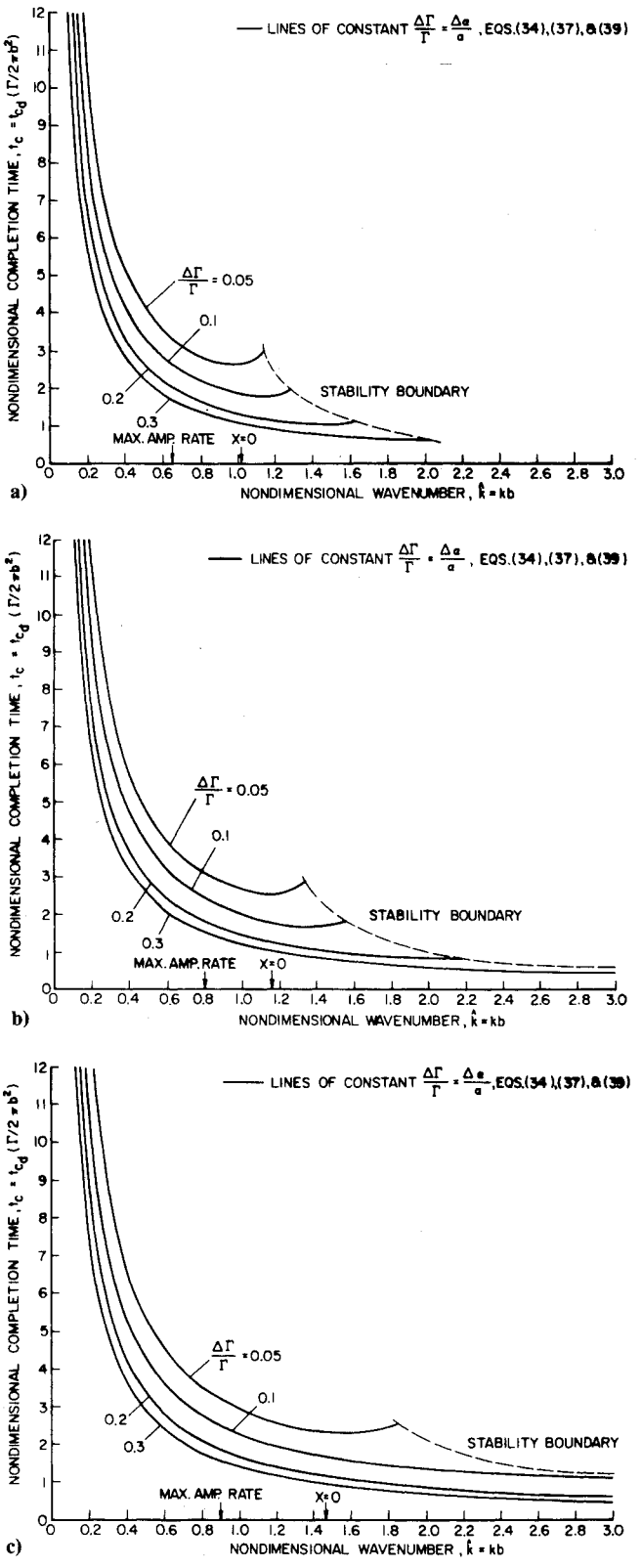

Fig. 5 Nondimensional completion time vs wavenumber for the case of forcing due to disturbances in the fluid, shown for various core sizes and forcing levels. a) Nondimensional effective vortex core size $a_e/b = 0.05$. b) Nondimensional effective vortex core size $a_e/b = 0.1$. c) Nondimensional effective vortex core size $a_e/b = 0.2$.

The above form is essentially the same as Eq. (32a). It follows that

$$t_c\Big|_{\omega=0} = (1/\sqrt{XY})\cosh^{-1}[X/2V_d+1] \qquad (42)$$

As before, this result applies when $X>0$, the case of hyperbolic trajectories. Corresponding results are obtained in the wavenumber range for which the trajectories are parabolic and elliptical by using V_d in place of Q_u in Eqs. (36-39). Figure 6 shows the completion time curves for the sinusoidal instability forced by a spatially periodic time-independent vertical velocity disturbance embedded in the fluid. These curves differ from those of Fig. 5 because V_d is independent of wavenumber, whereas Q_u does have a wavenumber dependence.

The other solvable case occurs when the argument of the hyperbolic functions in Eq. (40) must become large to achieve $x=\frac{1}{2}$. Under this condition, $\cosh\sqrt{XY}t \simeq \exp\sqrt{XY}t \gg 1$ and $\sinh\sqrt{XY}t \equiv \exp\sqrt{XY}t \gg 1$, when $t\to t_c$. After neglecting $e^{i\omega t}$ compared to $\exp\sqrt{XY}t$, a brief calculation gives

$$|x|\Big|_{t\to t_c} \simeq \frac{V_d}{2X}\frac{1}{\sqrt{1+\omega^2/XY}}e^{\sqrt{XY}t} \qquad (43)$$

The completion time is then found to be

$$t_c = (1/\sqrt{XY})\ln[(X/V_d)\sqrt{1+\omega^2/XY}] \qquad (44)$$

Equation (44) can be reconciled with Eq. (42) when $\omega=0$, provided the same simplifying assumptions are made. The form of Eq. (44) will always apply for V_d sufficiently small and $XY>0$ (hyperbolic trajectories). Again, the logarithmic dependence of completion time on the disturbance amplitude is apparent. The dependence on frequency is relatively weak unless the frequency is large compared to the reciprocal of the instability growth rate. In actual fact, frequency and wavenumber are related according to the nature of the disturbance in the fluid. Since the occurrence of sinusoidal instability is associated with large-scale disturbances which correspond to low frequencies in most physical processes, the frequency dependence shown in Eq. (44) may be unimportant in practice. Completion time curves for the sinusoidal instability forced by time-dependent disturbances imbedded in the fluid are also shown in Fig. 6. These curves are derived from Eq. (44). A comparison with the results from Eq. (42) for $\omega=0$ shows that Eq. (44) represents this limit with reasonable accuracy. An interesting feature of Fig. 6 is the rather weak dependence of completion time on the vortex core size.

Completion time calculations for time-dependent disturbances in the fluid could also be made without the simplifications embodied in Eqs. (43) and (44) by using an iterative numerical procedure. However, as long as the disturbance amplitudes are small, no dramatic changes are expected in the results as compared to the case for $\omega=0$.

The completion time curves shown in Figs. 5 and 6 exhibit several interesting features. The minimum completion time does not correspond to the wavenumber for the maximum amplification rate of the sinusoid amplitude when forcing is present. The minimum completion time actually occurs at a higher wavenumber because the vortex trajectory is shorter, as is clear from Fig. 4. As the vortex core size is increased, or as the level of forcing increases, this difference in wavenumbers becomes substantial. Since the angle θ of the vortex plane remains nearly constant in the unforced instability,[2] the issue of trajectory length never arises. Although the difference between wavenumbers for the maximum amplification rate and minimum completion time can be large, there is much less difference in the completion times. The results show the dependence of completion time on

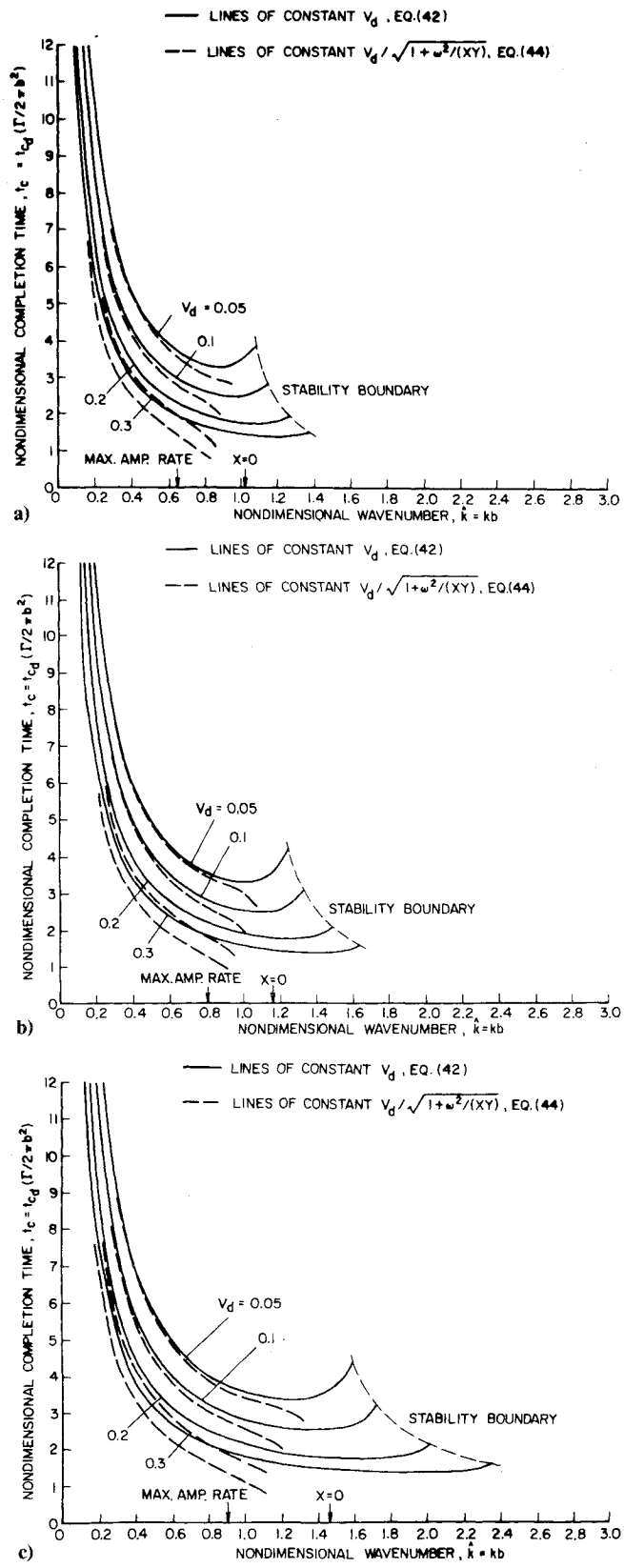

Fig. 6 Nondimensional completion time vs wavenumber for the case of forcing due to disturbances in the fluid, shown for various core sizes and forcing levels. a) Nondimensional effective vortex core size $a_e/b=0.05$. b) Nondimensional effective vortex core size $a_e/b=0.1$. c) Nondimensional effective vortex core size $a_e/b=0.2$.

wavenumber to be relatively weak for wavenumbers above the point of maximum amplification. Consequently, a broad range of disturbance wavenumbers are almost equally effective in bringing the instability to completion, particularly

when either the vortex core size or the forcing amplitude is large.

The stability boundary is defined as the wavenumber beyond which the vortex trajectories do not intersect. Beyond this wavenumber the sinusoidally disturbed vortices rotate periodically about their axes, their motion being dominated by self-induction. In the unforced case the stability boundary occurs at the wavenumber such that $X=0$; this point is indicated for each part of Figs. 5 and 6. The presence of forcing moves the stability boundary to larger wavenumbers, the displacement being greater when either the vortex core size or the forcing amplitude is increased. Again, it is clear that the presence of forcing extends the range of wavenumbers over which the instability can occur.

Random Forcing

The case of the forcing terms for the sinusoidal instability having random temporal and/or spatial behavior is now considered. For forcing due to unsteady loading, this corresponds to the load fluctuations of the lifting surface being a random function of time with a known frequency spectrum. The approach is essentially a generalization of the previous results using Fourier transforms.

The horizontal component of displacement of a vortex is $x(z,t)$. Using the Fourier integral theorem,

$$x(z,t)=\int_{-\infty}^{+\infty} x(\hat{k},t)e^{i\hat{k}z}\mathrm{d}\hat{k} \tag{45}$$

and

$$x(\hat{k},t)=\frac{1}{2\pi}\int_{-\infty}^{+\infty} x(z,t)e^{-i\hat{k}z}\mathrm{d}z \tag{46}$$

For the present purpose the displacement used in previous sections, e.g., see Eq. (1), is really the transformed displacement $x(\hat{k},t)$. When the instability is forced by unsteady loading, the general displacement can be written as

$$x(z,t)=\int_{-\infty}^{+\infty} Q_u(\hat{k})F(\hat{k},t)e^{i\hat{k}z}\mathrm{d}\hat{k} \tag{47}$$

where using Eqs. (32a), (36a), and (38a) define

$$F(\hat{k},t)=\begin{cases}(\cosh\sqrt{X(\hat{k})\,Y(\hat{k})}\,t-1)/X(\hat{k}) & X(\hat{k})>0\\ \tfrac{1}{2}Y(\hat{k})t^2 & X(\hat{k})=0\\ (\cos\sqrt{-X(\hat{k})\,Y(\hat{k})}\,t-1)/X(\hat{k}) & X(\hat{k})=<0\end{cases} \tag{48}$$

A corresponding result for the case of forcing by time-independent (frozen) disturbances in the fluid is obtained using Eq. (41) with $\omega=0$:

$$x(z,t)\Big|_{\omega=0}=\int_{-\infty}^{+\infty} V_d(\hat{k},0)F(\hat{k},t)e^{i\hat{k}z}\mathrm{d}\hat{k} \tag{49}$$

The forcing of the instability due to a time-independent, spatially random disturbance imbedded in the fluid has already been considered by Crow and Bate,[9] who obtained the equivalent of Eq. (49) except that the exponential approximation Eq. (43) was used with $\omega=0$. They also showed that the mean square displacement can then be expressed in a simple manner. However, when Eq. (43) is used in place of Eq. (41) a difficulty occurs because the integrand then becomes singular at the wavenumber for which $X=0$. Since the previous results have shown that the stability boundary lies beyond this wavenumber when forcing is present, and since the minimum completion time for a single wavenumber disturbance lies in this range, rather than at the maximum amplification point, the exponential approximation should not be used. This difficulty did not become apparent in the work of Ref. 9 because the method of steepest descents was used to evaluate the integral, and thus only the contribution in the vicinity of the wavenumber for maximum amplification was obtained. As a practical matter, this means that the actual completion times due to random forcing by fluid turbulence will be shorter than they predicted, since all wavenumbers from the maximum amplification point to the stability boundary will contribute significantly to the horizontal displacement of the vortex.

Following the approach of Ref. 9, adapted to the case of unsteady loading, the spatially averaged mean square displacement can be expressed in a simple manner:

$$\overline{x_u^2}=\int_0^{\infty} W_u(\hat{k})F(\hat{k},t)^2\mathrm{d}\hat{k} \tag{50}$$

where $W_u(k)$ is the one-sided power spectrum of Q_u, the velocity field induced by unsteady lift variations. Using Eq. (26) this quantity can be reexpressed as

$$W_u(\hat{k})=\frac{W_\Gamma(\hat{k})}{\Gamma^2}\left[V_v(\hat{k})+V_c(\hat{k})\right]^2 \tag{51}$$

where W_Γ is the power spectrum of the circulation variation in the wake. If $W_\alpha(f_u)$ is the power spectrum of the angle-of-attack variations which cause the lift variations, then the relations $\Delta\alpha/\alpha=\Delta\Gamma/\Gamma$ and $f_u=kU/2\pi$ can be used to reexpress Eq. (50) as

$$W_u(\hat{k})=(1/\alpha^2)\,W_\alpha(\hat{k}U/2\pi b)\left[V_v(\hat{k})+V_c(\hat{k})\right]^2 \tag{52}$$

The corresponding result for random forcing due to a time-dependent, spatially random disturbance imbedded in the fluid is

$$\overline{x_d^2}=\int_0^{\infty} W_d(\hat{k},0)F(\hat{k},t)^2\mathrm{d}k \tag{53}$$

where $W_d(\hat{k},0)$ is the one-sided power spectrum of the vertical velocity component of the disturbance field.

For either of the cases represented by Eqs. (50) or (53) the problem is to find the time for which the mean squared value is such that the instability is considered to be complete. Crow and Bate[9] made the somewhat conservative assumption that $\overline{x(t_c)^2}=1$ defines the completion time in the case of random forcing. Once this convention has been adopted, and the spectrum of fluid disturbances or of unsteady loading has been prescribed, then one approach is to perform the integration numerically and find t_c by iteration.

Concluding Remarks

The response of the sinusoidal instability of a vortex wake to forcing caused by unsteady loading or by disturbances embedded in the fluid has been determined. Solutions were obtained under the assumption that a linearized small perturbation analysis can adequately represent the process. An important aspect of the present work is the specification of initial conditions, thereby leading to the prediction of a definite completion time at which the opposite vortices come into contact. Both the cases of discrete and random forcing have been considered. Nondimensional completion time curves were generated for the discrete forcing cases. Calculation of the response to random forcing requires the specification of the spectrum of the parameter characterizing the level of forcing. The behavior of the forced instability is somewhat different than that of the unforced case. In par-

ticular, the forced instability can go to completion at wavenumbers larger than those for which the unforced case is stable. It was also found that the minimum completion time did not correspond to the wavenumber for which the amplification rate is a maximum, because the length of the vortex trajectories is also an important factor.

It is now possible to make statistical predictions of wake lifetime, given the appropriate spectra to characterize the unsteady loading and the atmospheric turbulence. The effect of vertical displacement of the wing, which introduces nontrivial initial conditions, should also be included. This can be done in a straightforward manner, given the wavenumber spectrum of the vertical displacement. A knowledge of the aircraft dynamics is required to determine the spectra of unsteady loading and vertical displacement in terms of the inputs from the atmosphere and the pilot.

Acknowledgment

This research was supported by a contract from Aeronautical Research Associates of Princeton, Inc.

References

[1]Crow, S.C., "Stability Theory for a Pair of Trailing Vortices," *AIAA Journal,* Vol. 8, Dec. 1970, pp. 2172-2179.

[2]Bliss, D.B., "The Dynamics of Curved Rotational Vortex Lines," M.S. thesis, Department of Aeronautics and Astronautics, MIT, Sept. 1970.

[3]Widnall, S.E., Bliss, D.B., and Zalay, A., "Theoretical and Experimental Study of the Stability of a Vortex Pair," *Aircraft Wake Turbulence and Its Detection,* edited by Olsen, J., Goldberg, A., and Rogers, M., Plenum Press, New York, 1971, pp. 305-338.

[4]Moore, D.W. and Saffman, P.G., "The Motion of a Vortex Filament with Axial Flow," *Philosophical Transactions of the Royal Society of London,* Vol. 272, July 1972, pp. 403-429.

[5]Widnall, S.E., "The Stability of Helical Vortex Filaments," *Journal of Fluid Mechanics,* Vol. 54, Part 4, 1972, pp. 641-663.

[6]Widnall, S.E. and Bliss, D.B., "Slender Body Analysis of the Motion and Stability of a Vortex Filament Containing an Axial Flow," *Journal of Fluid Mechanics,* Vol. 50, Part 2, 1971, pp. 335-353.

[7]Bilanin, A.J. and Widnall, S.E., "Aircraft Wake Dissipation by Sinusoidal Instability and Vortex Breakdown," AIAA Paper 73-107, Washington, D.C., 1973.

[8]Chevalier, H., "Flight Test Studies of the Formation and Dissipation of Trailing Vortices," *Journal of Aircraft,* Vol. 10, Jan. 1973, pp. 14-18.

[9]Crow, S.C. and Bate, E.R. Jr., "Lifespan of Vortices in a Turbulent Atmosphere," *Journal of Aircraft,* Vol. 13, July 1976, pp. 476-482.

[10]Moore, D.W., "Finite Amplitude Waves on Aircraft Trailing Vortices," Air Force Office of Scientific Research, Rept. AFOSR-TR-72-0033, Oct. 1971.

[11]Condit, P.M. and Tracy, P.W., "Results of the Boeing Company Wake Turbulence Test Program," *Aircraft Wake Turbulence and Its Detection,* edited by Olsen, J., Goldberg, A., and Rogers, M.H., Plenum Press, New York, 1971, pp. 489-492.

[12]Erdelyi, A., ed., *Tables of Integral Transforms,* Vol. I, (Bateman Manuscript Project), McGraw-Hill Book Company, Inc., New York, 1954.

[13]Boyce, W.E. and DiPrima, R.C., *Elementary Differential Equations and Boundary Value Problems,* 3rd ed. Chap. 7, John Wiley and Sons, New York, 1977.